Desta et al. International Journal of Mechanical and Materials Engineering (2021) 16:13
https://doi.org/10.1186/s40712-021-00135-5

International Journal of Mechanical and Materials Engineering

ORIGINAL PAPER Open Access

Microstructural and mechanical studies of feedstock material in continuous extrusion process

Tariku Desta, Devendra Kumar Sinha*, Perumalla Janaki Ramulu and Habtamu Beri Tufa

Abstract

The challenge encountered in continuous forming process is the variation in mechanical strength of product formed with respect to process variables like extrusion wheel speed and diameter of product. In this research article, the micro-structural investigation of the aluminum (AA1100) feedstock material of 9.5-mm diameter has been carried out at various extrusion wheel speeds and diameter of product before and after deformation on commercial continuous extrusion setup TBJ350. The mechanical properties like yield strength as well as percentage elongation have been estimated and optimized using two variables with 3 levels through central composite rotatable design (CCRD) method. The mathematical modeling has been carried out to predict the optimum combination of process parameters for obtaining maximum value of yield strength and percentage elongation. The statistical significance of mathematical model is verified through analysis of variance (ANOVA). The optimum value of yield strength is found to be 70.939 MPa at wheel velocity of 8.63 rpm and product diameter of 9 mm respectively, whereas the maximum percentage elongation recorded is 46.457 at wheel velocity of 7.06 rpm and product diameter of 7.18 mm. The outcome may be useful in obtaining the best parametric combination of wheel speed and extrusion ratio for best strength of the product.

Keywords: Continuous forming extrusion, Central composite rotatable design, Analysis of variance, Microstructures, Pure Aluminum AA1100

Introduction

The demands of continuous profiles of the product for various engineering applications are increasing day by day. The main limitation of conventional extrusion process is that only finite profiles of the product can be formed. The continuous forming process is one through which infinite lengths of product can be formed with high dimensional accuracy and excellent metallurgical and mechanical properties. The continuous forming process known as CONFORM process was started by British Atomic Energy Department (Bridewater & Maddock, 1992; Green, 1972). Figure 1 shows the principle of continuous forming extrusion process along with the tooling used.

The numerical investigation of the process variables was carried out through DEFORM-3D to determine the flow behavior of the material, strain effective, and temperature distribution (Kim et al., 1998). The upper bound technology for estimation of power required for the deformation of feedstock material from the entry of feedstock to the die exit was applied. The theoretical results were validated with numerical simulation results and were found in good agreement (Cho et al., 2000). The investigation of flash formation was carried out for copper feedstock material in continuous extrusion forming process under different frictional conditions (Manninen et al., 2006a). The analytical model was developed in order to analyze the mechanics behind the flash formation. The relationship was established among flash formation, extrusion pressure, friction, and flash gap size

* Correspondence: ds3621781@gmail.com
MDME, SoMCME, Adama Science & Technology University, Adama, Ethiopia

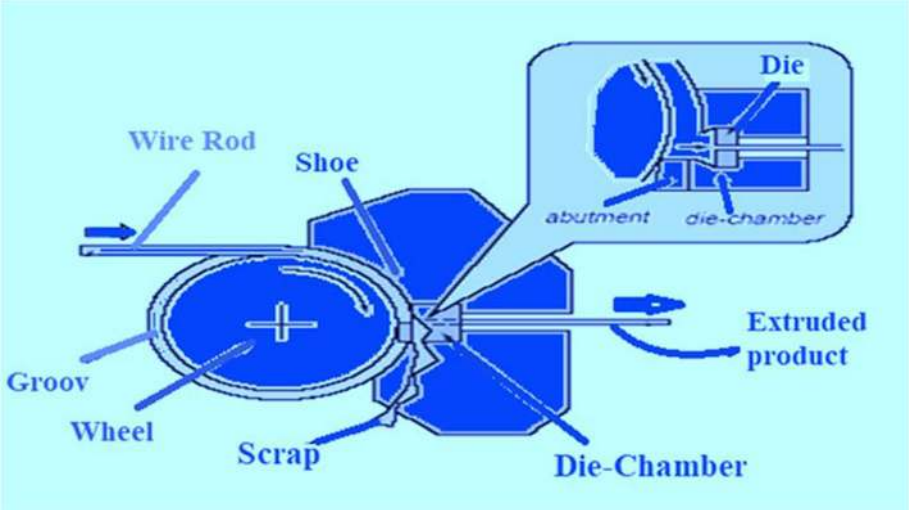

Fig. 1 Principle of continuous extrusion process

(Manninen et al., 2006b). The development of mathematical model was carried out for prediction and estimation of various distributions of process characteristics such as temperature, effective stresses, and effective strains for the feedstock material. Important information regarding process control and optimization was provided (Lu et al., 1998). It was observed that the tool geometry affects the flow behavior of the material and process conditions in continuous extrusion forming process. Therefore, streamline tool designs are recommended (Manninen et al., 2010). For improvement of product quality, sensing and control mechanism was developed (Khawaja et al., 2005; Khawaja & Seneviratne, 2001) and (Khawaja et al., 2004). Parametric investigation for analysis of surface defect and curling phenomenon was carried out analytically and numerically (Cho & Jeong, 2000; Cho & Jeong, 2001; Cho & Jeong, 2003). The influence of wheel speed for analysis of effective stresses, effective strains, temperature field, and damage field were investigated during production of copper bus bar in continuous extrusion forming process (Peng-yue et al., 2007). The optimum value of wheel velocity was determined for enhancement in the quality of grain size and grain growth for AA 6063 feedstock material in continuous extrusion process (Zhao et al., 2013). The effect of feedstock temperature in continuous extrusion was carried out to analyze the optimum force needed for the deformation of feedstock material through the die exit (Sinha & Kumar, 2014). The extrusion wheel temperature, temperature of feedstock rod, and circumferential speed of extrusion wheel have significant impact on whole continuous extrusion process (Hodek et al., 2013; Hodek & Zemko, 2012) and (Zemko et al., 2013). Force analysis for the deformation of feedstock

Table 1 Input process variables and their levels

Factors	Levels of factor		
	−1	0	1
Wheel speed (rpm)	4	6	8
Product diameter (mm)	6	7	8

Table 2 List of experiments

Experiment No.	Wheel speed (revolutions per minute)		Diameter of product (mm)	
	Coded values	Actual values	Coded values	Actual values
1	− 2	1	0	7
2	1	10	1	8
3	− 1	4	1	8
4	0	7	0	7
5	0	7	− 2	5
6	0	7	0	7
7	2	13	0	7
8	− 1	4	− 1	6
9	0	7	0	7
10	1	10	− 1	6
11	0	7	2	9
12	0	7	0	7
13	0	7	0	7

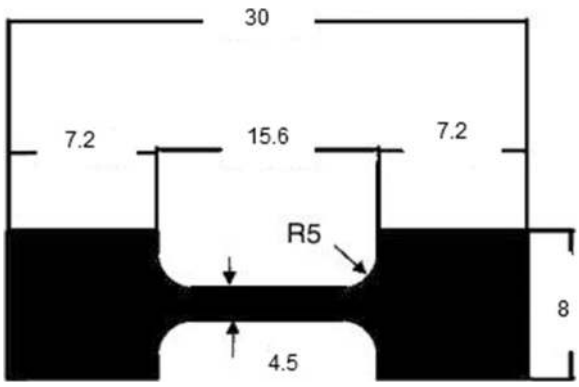

Fig. 2 Sample for tensile test (7 mm and 8 mm extruded aluminum rod, gauge length = 15.6 mm and gauge diameter = 4.5 mm)

material Al-Ti-B alloy was carried out using slab method (Cao et al., 2013). The investigation on recycling of titanium alloy powders and swarf through continuous extrusion into affordable wire for additive manufacturing was carried out. The continuous extrusion process was employed to consolidate waste titanium alloy feedstocks in the form of gas atomized powder and machining swarf into wire. It was found that almost 100% of the waste powder can be converted into wire by using conform process (Smythe et al., 2020). The investigation was carried out on the mechanical integrity of AA 6082 3D structures deposited by hybrid metal extrusion and bonding additive manufacturing. It was found that ultimate tensile strength approached that of the substrate material of the same alloy, yet with a somewhat lower elongation prior to facture (Blindheim et al., 2020).

The mathematical modeling and optimization of mechanical properties of copper (C101) feedstock in continuous extrusion process was carried out. The yield strength and % elongation of feedstock rod at different wheel velocities and product diameter was estimated (Sinha et al, 2018a). The optimization of process parameters such as wheel speed and extrusion ratio was carried out to optimize the mechanical properties such as ultimate tensile strength and hardness of continuously extruded feedstock rod of Aluminum alloy (Sinha et al, 2018b).

Based on the investigations carried out in continuous forming process in the past for pure metals like aluminum and copper, a mathematical modeling has been developed for the optimum values of mechanical properties, i.e., strength at yield point and elongation in percentage of the extruded material considering optimum values of the wheel speed and diameter of product. The microstructural analysis of material has also been carried out in this paper for pre and post deformation cases.

Materials and methodology

The continuous extrusion of aluminum alloy (AA1100) feedstock material is done through commercially available machine of continuous extrusion TBJ350. The raw material used for the investigation was circular rod of 9.5-mm diameter. The feedstock diameter of 9.5 mm has been extruded to product diameter of 6 mm, 7 mm, and 8 mm. The deformation of feedstock material has been carried out on extrusion wheel velocities of 4, 6, and 8 revolutions per minute (rpm). The experiments have been planned and performed on two factors and three levels CCRD using response surface methodology (RSM). Table 1 shows the levels of wheel velocities and product diameter used for carrying out the experiments.

A total of 13 experiments shown in Table 2 were performed for analysis of metallurgical and mechanical properties of the feedstock material before and after

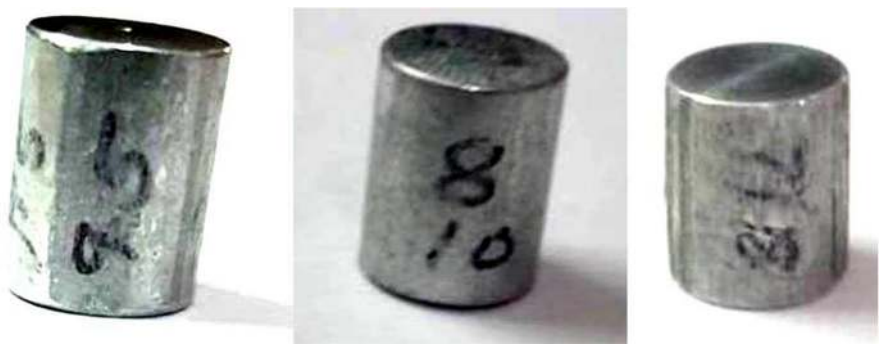

Fig. 3 Samples for analysis of microstructure before extrusion **a** 9.5 mm and after extrusion **b** 8 mm and **c** 7mm

Table 3 List of experiments for the analysis of yield strength

Experiment No.	Wheel velocity (rpm)		Product diameter (mm)		Yield strength (MPa)
	Coded values	Actual values	Coded values	Actual values	
1	− 2	1	0	7	18
2	1	10	1	8	51.5
3	− 1	4	1	8	42.75
4	0	7	0	7	33
5	0	7	− 2	5	65
6	0	7	0	7	33
7	2	13	0	7	18
8	− 1	4	− 1	6	36.2
9	0	7	0	7	33.
10	1	10	− 1	6	39.67
11	0	7	2	9	65
12	0	7	0	7	33
13	0	7	0	7	33

deformation process. The tensile test sample is shown in Fig. 2.

The samples for tensile test have been prepared as per the ASTM standards of gauge length 15.6 mm and 4.5 mm as the gauge diameter. The tensile test has been carried out on Instron machine with strain rate of 1 mm per minute. The yield strength has been recorded and percentage elongation has been calculated. The mathematical modeling of the yield strength and percentage elongation has been carried out using RSM. The significance of the developed mathematical model has been tested through analysis of variance method.

The analysis of microstructure of Aluminum AA1100 material has been carried out using optical microscopy. The samples initially were rubbed using emery papers of various grades to get mirror like surface. The polishing of the samples was carried out using Kerosene, Brasso, and cloth made of velvet. The etching of the samples was carried out using Keller's reagent. After sufficient etching, the samples were mounted on slides under the microscope for getting the microstructures of the samples.

The equation for measuring the grain size of the microstructure is given as (Underwood, 1970):

$$d = \left(L_{\text{avg}}.\text{grain shape factor}\right)/M \tag{1}$$

where d and M are the diameter of grain and magnification respectively.

The samples prepared for microstructure analysis are shown in Fig. 3.

Results and discussions

Mathematical modeling of yield strength

The tensile tests were carried out as per the experimental design at various wheel velocities and product diameter. Table 3 shows the experimental result of yield strength.

The significance of the input process variables, i.e., wheel speed and diameter of product, is shown in Table 4. It can be observed that the quadratic effect of wheel speed as well as diameter of product are very much significant on yield strength of the material since the p-value is much less than 0.05 whereas the linear effect of input process variables are insignificant due to their p-values much greater than 0.05 at 95% confidence interval or 5% significance level. The R^2 value is found to be 95.96% whereas adjusted R^2 value is found to be 93.07%.

The mathematical regression model as per Table 4 is written as:

$$\text{Yield strength } (Y) = 35.12 - 0.935X_1 - 1.4483X_2 - 3.6547X_1^2 + 1.57X_1X_2 \tag{2}$$

It can be observed from Table 5 that Fisher's test value for treatment combination of quadratic term is 53.62.

Table 4 Significance test of yield strength

Treatment combinations	Co-efficient	t-value	p-value
Constant	35.12	16.7	0.001
Wheel velocity (X_1)	0.9350	0.687	0.514
Product diameter (X_2)	1.4483	1.064	0.323
Wheel velocity × wheel velocity (X_1^2)	−3.6547	−3.710	0.008
Product diameter × product diameter (X_2^2)	8.0953	8.217	0.000
Wheel velocity × product diameter (X_1X_2)	1.5700	0.666	0.527

Table 5 Analysis of variance for yield strength

Sources of variation	Degree of freedom	Square sum	Mean square sum	Fishers test value	p-value
Regression	5	2430.48	486.10	21.86	0.000
Linear	2	35.66	35.66	0.80	0.486
Square	2	2384.96	1192.48	53.62	0.000
Interaction	1	9.86	9.86	0.44	0.527
Residual error	7	155.69	22.24		
Lack of fit	3	155.69	51.90		
Pure error	4	0.00	0.00	0.00	
Total	12	2586.17			

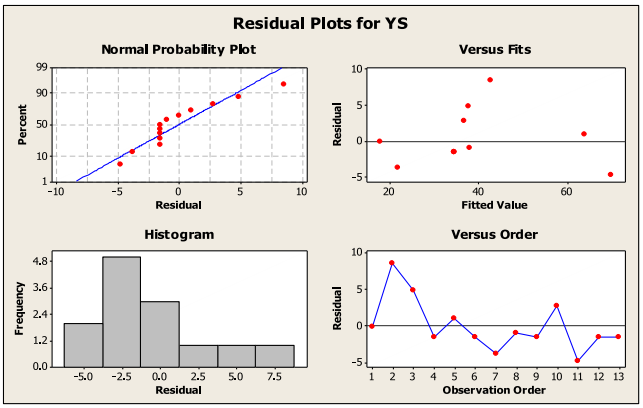

Fig. 4 Probability plot of residual for yield strength

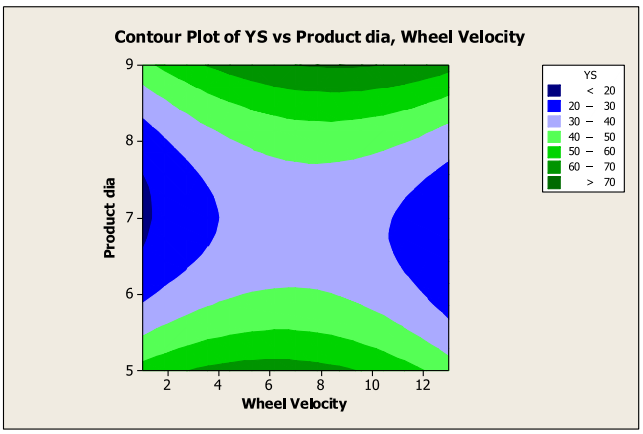

Fig. 5 Effect of wheel speed and diameter of product on yield strength in contour form

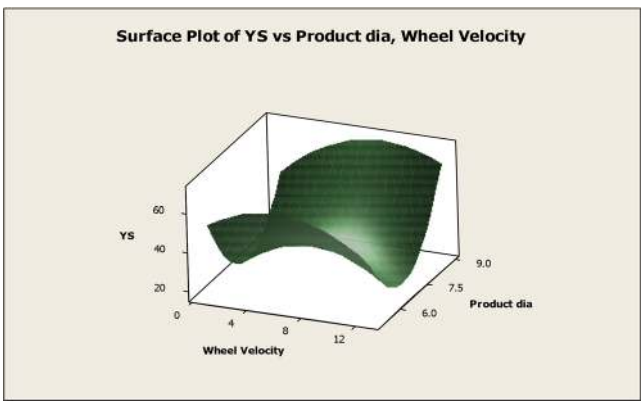

Fig. 6 Effect of wheel speed and diameter of product on yield strength in surface form

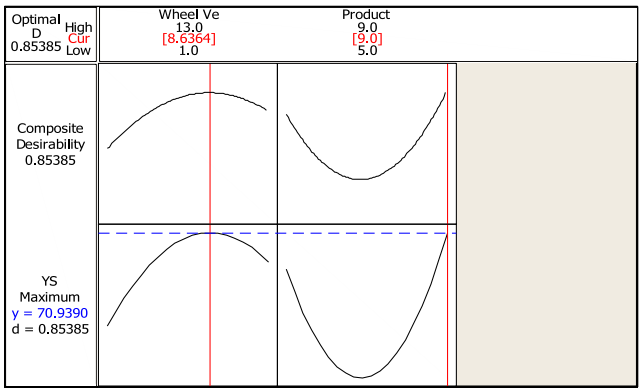

Fig. 7 Optimized value of yield strength in terms of wheel speed and diameter of product

Therefore, the quadratic effect of wheel speed and diameter of product is significant statistically. The regression value of 21.86 represents the Fisher test value for the mathematical model shown by Eq. (2). The value of 21.86 shows that the mathematical model developed is significant.

Figure 4 shows the plot of residuals for yield strength. It can be observed that data are uniformly distributed across the fitted line. Therefore, the model is said to be adequate.

Figures 5 and 6 show the effect of input process variables, i.e., the wheel speed and diameter of product on yield strength value of the extruded material in the form of contour and surface plots respectively. It can be observed from Fig. 5 that the yield strength value of 70MPa and greater can be achieved if the wheel speed is in the range of 3 to 9 rpm whereas the diameter of product is around 5 mm. The surface plot signifies that the value of yield strength initially decreases, becomes minimum, and then increases with further increase in the values of input process variables.

From Fig. 7, it can be observed that the maximum value of yield strength of 70.93 MPa can be obtained if the value of wheel speed is 8.6364 rpm and diameter of product is 9 mm.

The effect of wheel speed on 0.2% yield strength of extruded product is shown in Fig. 8. It can be observed that if the wheel speed increases, the yield strength of product increases and it is maximum at a given value of wheel speed and decreases thereafter if wheel speed is increased further.

The effect of extrusion ratio on yield strength is shown in Fig. 9. As the extrusion ratio increases, the yield strength value of the extruded product samples decreases initially, becomes minimum at a given extrusion ratio at a given speed, and increases thereafter.

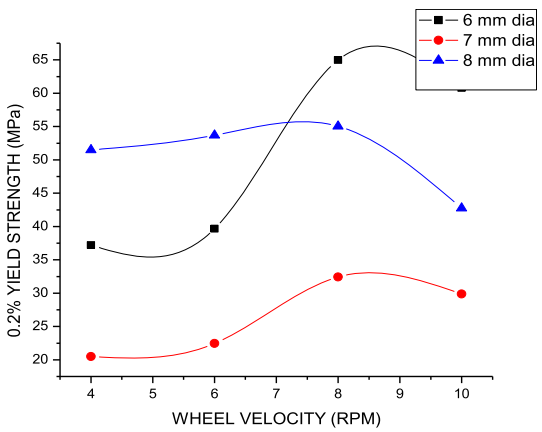

Fig. 8 Variation of 0.2% yield strength with extrusion wheel velocity

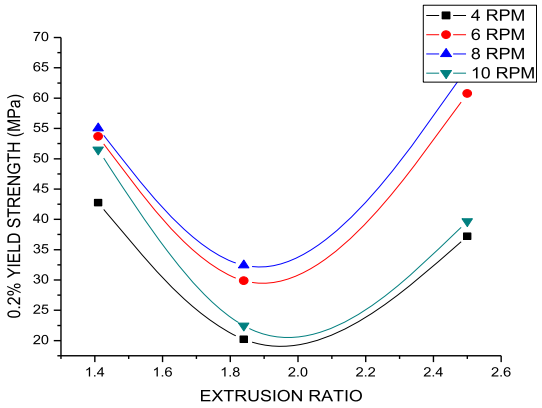

Fig. 9 Variation of 0.2% yield strength with extrusion ratio

Mathematical modeling of percentage elongation

Table 6 shows the list of experiments carried out for analysis of % elongation.

The significance of the input process variables, i.e., wheel speed and diameter of product, is shown in Table 7. It can be observed that the quadratic effect of wheel speed as well as diameter of product is very much significant on yield strength of the material since the *p*-value is much less than 0.05 whereas the linear effect of input process variables are insignificant due to their *p*-values much greater than 0.05 at 95% confidence interval or 5% significance level. The R^2 value is found to be 96.67% whereas adjusted R^2 value is found to be 96.15%.

The mathematical regression model as per Table 7 is written as:

$$L = 46.3973 - 0.25X_1 + X_2 - 5.82X_1^2 - 3.2575X_2^2 + 3X_1X_2 \quad (3)$$

It can be observed from Table 8 that Fisher's test value for treatment combination of quadratic term is 144.16 whereas for interaction effect is 12.35. Therefore, the quadratic and interaction effect of wheel speed and diameter of product on % elongation of extruded product is significant statistically. The regression value of 61.01 represents the Fisher test value for the

Table 6 List of experiments for analysis of % elongation

Experiment No.	Wheel velocity (rpm)		Product diameter (mm)		% Elongation
	Coded values	Actual values	Coded values	Actual values	
1	− 2	1	0	7	25.5
2	1	10	1	8	43.0
3	− 1	4	1	8	34.0
4	0	7	0	7	46.5
5	0	7	− 2	5	32.0
6	0	7	0	7	46.5
7	2	13	0	7	21.0
8	− 1	4	− 1	6	36.0
9	0	7	0	7	46.5
10	1	10	− 1	6	34.0
11	0	7	2	9	35.0
12	0	7	0	7	46.5
13	0	7	0	7	46.5

Table 7 Significance test of % elongation

Term	Co-efficient	*t*	*p*
Constant	46.3793	65.424	0.000
Wheel velocity (X_1)	− 0.2500	− 0.507	0.628
Product diameter (X_2)	1.0000	2.029	0.082
Wheel velocity × wheel velocity (X_1^2)	− 5.8200	− 16.318	0.000
Product diameter × product diameter (X_2^2)	− 3.2575	− 9.134	0.000
Wheel velocity × product diameter (X_1X_2)	3.0000	3.514	0.010

mathematical model shown by Eq. (3). The value of 61.01 shows that the mathematical model developed is significant.

Figure 10 shows the plot of residuals for % elongation. It can be observed that data are uniformly distributed across the fitted line. Therefore, the model is said to be adequate.

Figures 11 and 12 show the effect of input process variables, i.e., the wheel speed and diameter of product on yield strength value of the extruded material in the form of contour and surface plots respectively. It can be observed from Fig. 11 that % elongation is greater than 40 if the wheel speed lies in the range of 4 to 10 rpm whereas the range of diameter of product is from 5.75 to 8.75mm.

The surface plot of Fig. 12 signifies that % elongation of the extruded material increases with the increase in the values of wheel speed and diameter of product and is maximum at a given value of wheel speed and diameter of product and decreases thereafter with further increment in the values of wheel speed and diameter of product. From Fig. 13, it can be inferred that the maximum value of 46.457% can be achieved at wheel speed of 7.06 rpm and 7.18 diameter of product.

Figure 14 shows the variation of % elongation with extrusion wheel velocity for aluminum alloy. It can be analyzed that % elongation increases with the increase in the value of wheel speed and becomes maximum at a given value of wheel speed for each value of extrusion ratio and decreases thereafter.

Figure 15 shows the variation of % elongation with extrusion ratio for aluminum alloy. It can be analyzed that % elongation increases with increase in the value of extrusion ratio and becomes maximum at a given value of extrusion ratio for each value of wheel speed and decreases thereafter.

Table 8 Analysis of variance for % elongation

Source	DF	Sum of squares	Mean sum of squares	*F*-value	*p*-value
Regression	5	889.097	176.819	61.01	0.000
Linear	2	12.750	6.375	2.19	0.183
Square	2	840.347	420.173	144.16	0.00
Interaction	1	36.000	36.00	12.35	0.010
Residual error	7	20.403	2.915		
Lack of fit	3	20.403	6.801		
Pure error	4	0.00	0.00		
Total	12	909.50			

Microstructure analysis

The microstructural analysis of the aluminum alloy AA 1100 has been done under various wheel speed and extrusion ratio. It has been observed that before deformation there is no change in grain size but after deformation, the elongations in grains are observed. The average grain size of the extruded product was found to be *80 to 200 μm* under wheel speed of 6 to 10 revolutions per minute. Therefore, the grains were larger and non-homogeneous. But under the wheel speed of 8 revolutions per minute, very fine and uniform grains were observed. The further increase in wheel speed slightly increased the grain size. Figures 16, 17, 18, 19, 20, 21, 22, and 23 show the microstructures of aluminum samples at various wheel velocities and extrusion ratio.

Conclusions

The optimization of the continuous extrusion process parameters for aluminum alloy (AA 1100) feedstock materials was done using response surface methodology to determine the best possible process parameters (wheel speed and diameter of product) for process controls. To help the industries in the area of continuous extrusion for achieving best possible properties of extruded feedstock as well as to produce defect free products with better surface quality and strength, the optimal value of best CE process parameters have been predicted. The optimized value of input process variables of wheel speed and diameter of product were found to be 8.63 revolutions per minute and 9 mm as diameter of product respectively for yield strength 70.939 MPa. The optimized value of input process variables, i.e., the wheel speed and diameter of product, was found to be 7.06 revolutions per minute and 7.18 diameter of product respectively for maximum percentage elongation of 46.447. The average grain size of the extruded product was found to be 80 to 200 μm under wheel speed of 4 to 10 revolutions per minute. Therefore, the grains were larger and non-homogeneous. But under the wheel speed of 8 revolutions per minute, very fine and uniform grains were observed. The further increase in wheel speed slightly increased the grain size. The present investigation may be helpful in achieving best combination of wheel speed and extrusion ratio for better quality of extruded product.

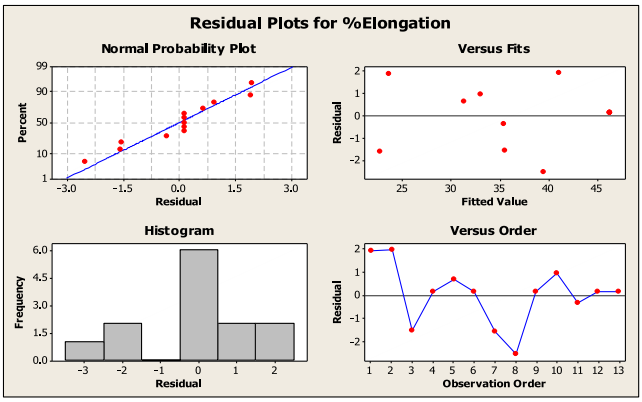

Fig. 10 Probability plot of residual for % elongation

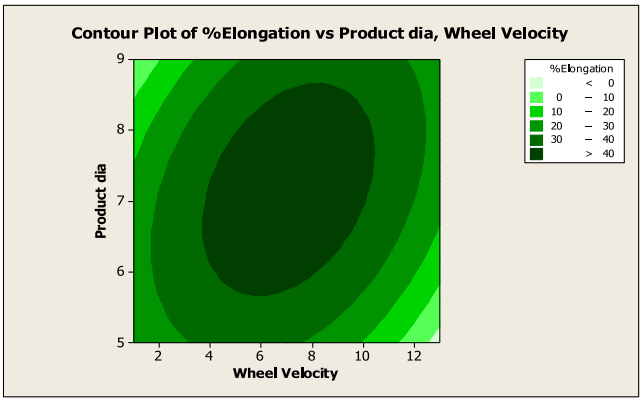

Fig. 11 Effect of wheel speed and diameter of product on % elongation in contour form

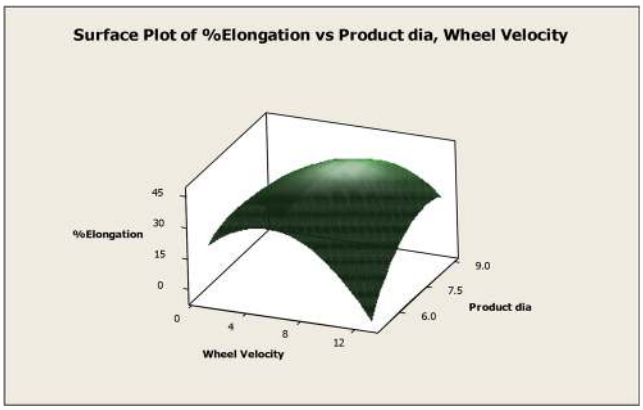

Fig. 12 Effect of wheel speed and diameter of product on % elongation in surface form

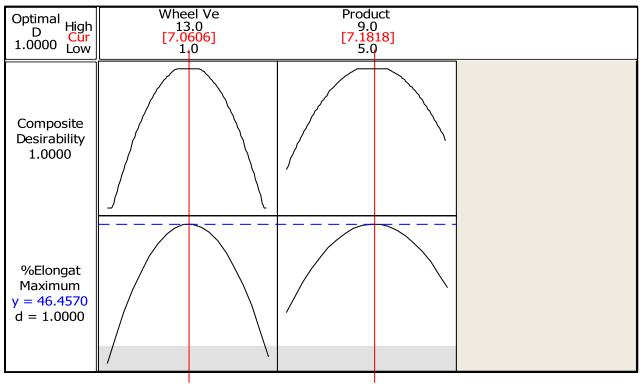

Fig. 13 Optimized value of yield strength in terms of wheel speed and diameter of product

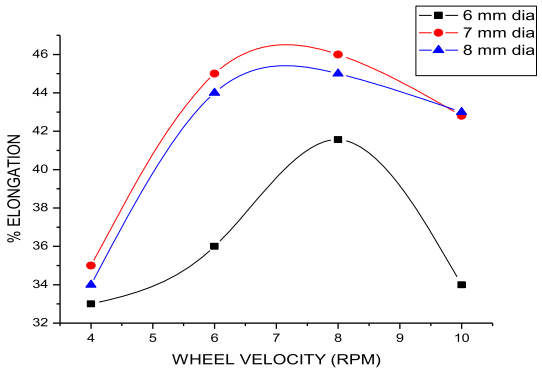

Fig. 14 Variation of % elongation with extrusion wheel velocity

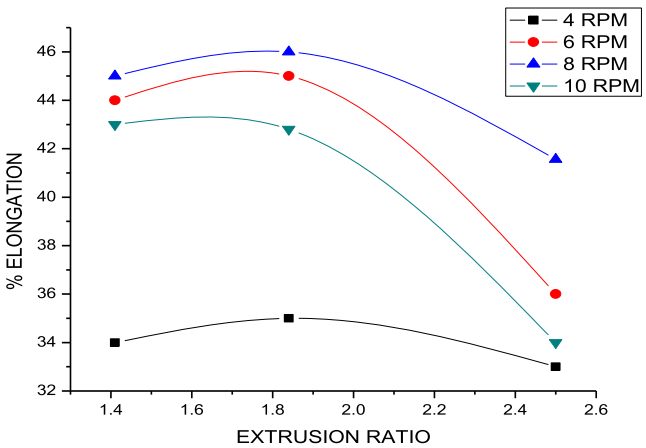

Fig. 15 Variation of % elongation with extrusion ratio or product diameter

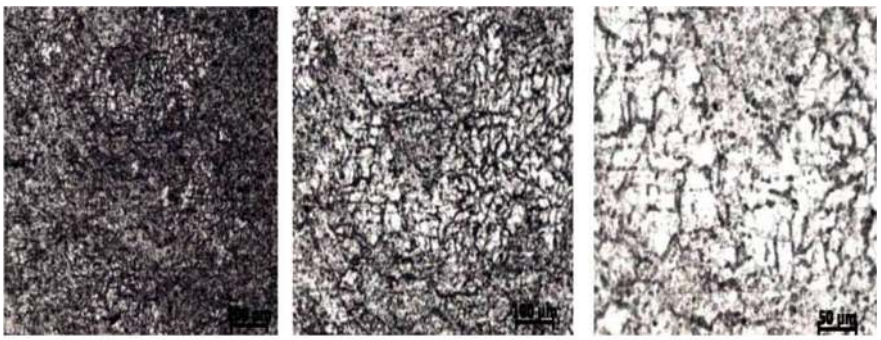

(a) (c) (b)

Fig. 16 a–c Micrographs of aluminum at 6 mm, 6 rpm at 50× magnification, 100× magnification, and 200× magnification respectively

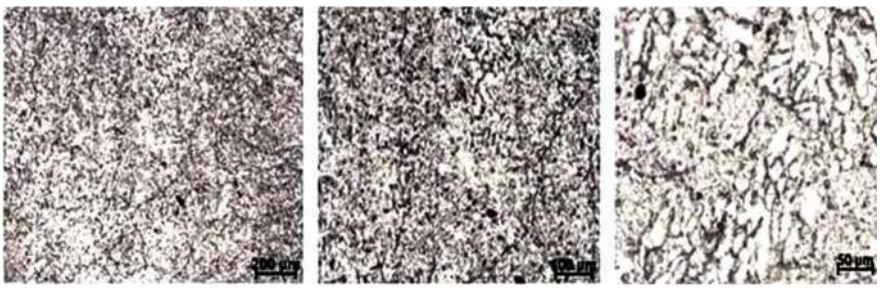

(a) (b) (c)

Fig. 17 a–c Micrographs of aluminum at 7 mm, 6 rpm at 50×, 100×, and 200× magnification respectively

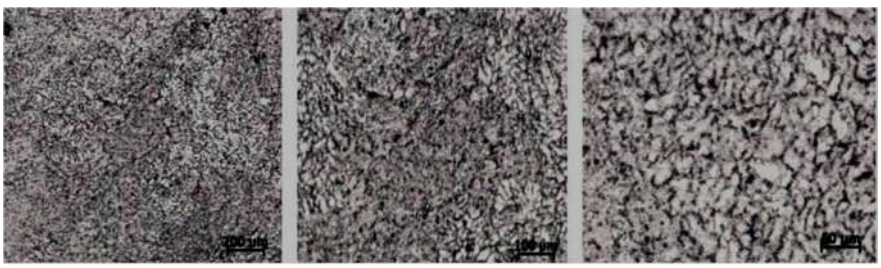

(a) (b) (c)

Fig. 18 a–c Micrographs of aluminum at 8 mm, 6 rpm at 50× magnification, 100× magnification, and 200× magnification respectively

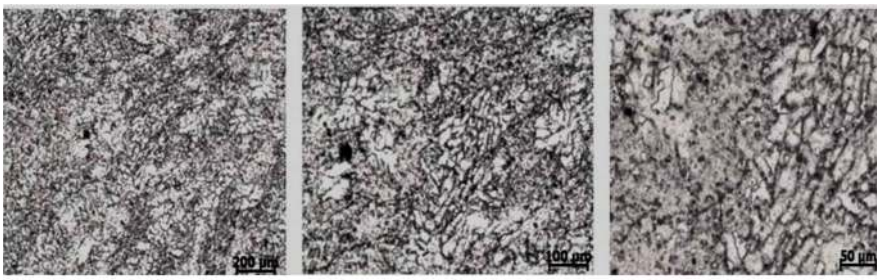

(a) (b) (c)

Fig. 19 a–c Micrographs of aluminum at 6 mm, 8 rpm at 50×, 100×, and 200× magnification respectively

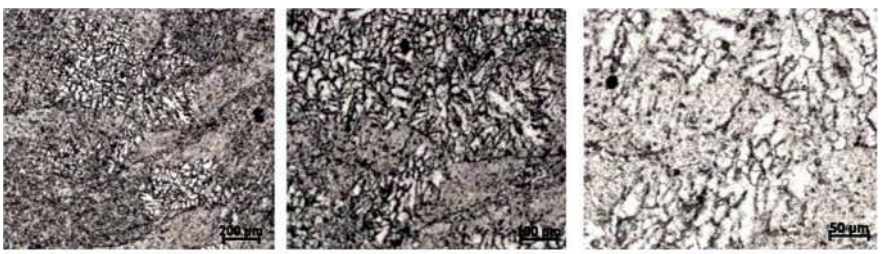

(a) (b) (c)

Fig. 20 a–c Micrographs of aluminum at 7 mm, 8 rpm at 50×, 100×, and 200× magnification respectively

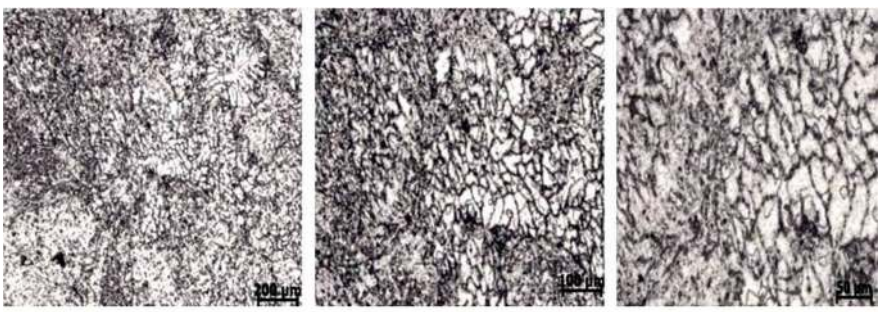

(a) (b) (c)

Fig. 21 a–c Micrographs of aluminum at 8 mm, 8 rpm at 50×, 100×, and 200× magnification respectively

Fig. 22 a–c Micrographs of aluminum at 8 mm, 10 rpm at 50×, 100×, and 200× magnification respectively

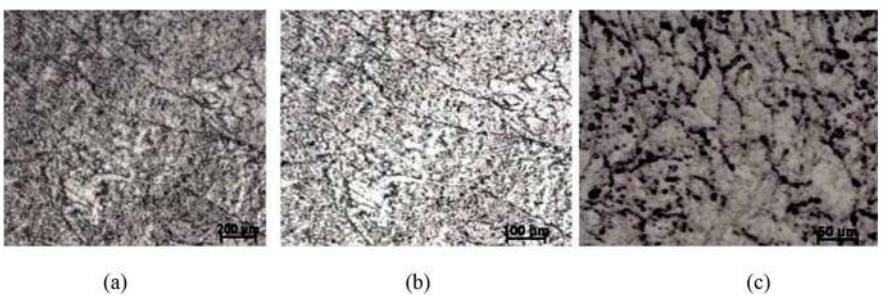

Fig. 23 a–c Micrographs of aluminum at 9.5 mm, 6 rpm at 50×, 100×, and 200× magnification respectively

Acknowledgements
Not applicable.

Authors' contributions
Tariku Desta: Investigation, writing original draft. *Devendra Kumar Sinha*: Writing, review and editing. *Perumalla Janaki Ramulu*: Proof reading and editing. *Habtamu Beri Tufa*: Supervision. The authors read and approved the final manuscript.

Funding
No funding has been done for this research work.

Availability of data and materials
The datasets used and/or analyzed during the current study are available from the corresponding author on reasonable request.

Declaration

Competing interests
The authors declare that they have no competing interest.

Received: 30 January 2021 Accepted: 15 August 2021
Published online: 06 September 2021

References

Blindheim, J., Grong, O., Welo, T., & Steinert, M. (2020). On the mechanical integrity of AA 6082 3D structures deposited by hybrid metal extrusion & bonding additive manufacturing. *Journal of Materials Processing Technology*, *282*, 116684. https://doi.org/10.1016/j.jmatprotec.2020.116684.

Bridewater, M., & Maddock, B. (1992). New developments in conform technology for continuous extrusion, Proceedings of the Fifth International Aluminium Extrusion Technology Seminar, Chicago, USA. *Aluminium Extruders Council and the Aluminium Association*, *1*, 413–419.

Cao, F., Wen, J., Ding, H., Wang, Z., Li, Y., Guan, R., & Hou, H. (2013). Force analysis and experimental study of pure aluminum and Al-5%Ti-1%B alloy continuous expansion extrusion forming processes. *Transactions of Nonferrous Metals Society of China*, *23*(1), 201–207. https://doi.org/10.1016/S1003-6326(13)62447-4.

Cho, J. R., & Jeong, H. S. (2000). Parametric investigation on the surface defect occurrence in CONFORM process by the finite element method. *Journal of Materials Processing Technology*, *104*(3), 236–243. https://doi.org/10.1016/S0924-0136(00)00572-0.

Cho, J. R., & Jeong, H. S. (2001). Parametric investigation on the curling phenomenon in CONFORM process by three-dimensional finite element analysis. *Journal of Materials Processing Technology*, *110*(1), 53–60. https://doi.org/10.1016/S0924-0136(00)00658-0.

Cho, J. R., & Jeong, H. S. (2003). CONFORM process: surface separation, curling and process characteristics to the wheel diameter. *Journal of Materials Processing Technology*, *136*(1-3), 217–226. https://doi.org/10.1016/S0924-0136(03)00164-X.

Cho, J. R., Kim, Y. H., Kim, K. S., Jeong, H. S., & Yoon, S. S. (2000). A study of the application of upper bound method to the CONFORM process. *Journal of Materials Processing Technology*, *97*, 153–157.

Green, D. (1972). Continuous extrusion of wire sections. *Journal of Institute of Metals*, *100*, 296–300.

Hodek, J., Kubina, T., & Dlouhy, J. (2013). FEM model of continuous extrusion of titanium in deform software. *METAL*, *5*, 15–17.

Hodek, J., & Zemko, M. (2012). FEM model of continuous extrusion of titanium in deform software. *COMAT*, *11*, 21–22.

Khawaja, K., Clode, M. P., Althoefer, K., & Seneviratne, L. (2004). Gap sensing benefits in conform™ extrusion machinery. In *IEEE, International Conference on Robotics and Automation Proceedings*.

Khawaja, K., Clode, M. P., & Seneviratne, L. (2005). Benefits of wheel-tool gap sensing in conform™ extrusion machinery. *IEEE/ASME International Conference on Mechatronics*, *I*, *10*, 4.

Khawaja, K., & Seneviratne, L. (2001). Sensing & control of conform™ extrusion gap between wheel and tooling plates, vol. 1. *IEEE/ASME International Conference on Advanced Intelligent Mechatronics Proceedings*, Como, pp 8–12.

Kim, Y. H., Cho, J. R., Kim, K. S., Jeong, H. S., & Yoon, S. S. (1998). A study on optimal design for CONFORM process. *Journal of Materials Processing Technology*, *80-81*, 671–675. https://doi.org/10.1016/S0924-0136(98)00173-3.

Lu, J., Saluja, N., Riviere, A. L., & Zhou, Y. (1998). Computer modelling of the continuous forming extrusion process of AA6061 alloy. *Journal of Materials Processing Technology*, *79*(1-3), 200–212. https://doi.org/10.1016/S0924-0136(98)00011-9.

Manninen, T., Katajarinne, T., & Ramsay, P. (2006a). Analysis of flash formation in continuous rotary extrusion of copper. *Journal of Materials Processing Technology*, *177*(1-3), 600–603. https://doi.org/10.1016/j.jmatprotec.2006.04.051.

Manninen, T., Katajarinne, T., & Ramsay, P. (2006b). Numerical simulation of flash formation in continuous rotary extrusion of copper. *Journal of Materials Processing Technology*, *177*, 604–607.

Manninen, T., Ramsay, P., & Korhonen, A. S. (2010). Three-dimensional numerical modeling of continuous extrusion. *Journal of Materials Processing Technology*, *177*, 600–603.

Peng-yue, W. U., Shui-Sheng, X., Hua-qing, L., Ming, Y., Guo-Jie, H., & Lei, C. (2007). Effect of extrusion wheel angular velocity on continuous extrusion forming process of copper concave bus bar. *Transactions of Nonferrous Metals Society of China*, *17*, 280–286.

Sinha, D. K., & Kumar, S. (2014). *Effect of feedstock temperature in continuous extrusion*. Guwahati: AIMTDR, IIT.

Sinha, D. K., Kumar, S., Kumar, A., & Yadav, A. (2018a). Mathematical modeling to predict mechanical properties of copper (C101) feedstock in continuous extrusion. *IOP Conference Series: Material Science and Engineering*, *404*, 012052(1–10).

Sinha, D. K., Kumar, S., Kumar, A., & Yadav, A. (2018b). Optimization of process parameters in continuous extrusion of aluminum alloy. In *International Conference on Computational and Characterization Techniques in Engineering and Science (CCTES)*.

Smythe, A. S., Thomas, M. B., & Jackson, M. (2020). Recycling of titanium alloy powder and swarf through continuous extrusion (Conform) into affordable wire for additive manufacturing. *Metals*, *10*(6), 843. https://doi.org/10.3390/met10060843.

Underwood, E. E. (1970). *Quantitative stereology*, 2nd ed., Addison-Wesley Publishing Company, Reading, MA.

Zemko, M., Hodek, J., Kraus, L., & Dlouhy, J. (2013). FEM modeling of continuous extrusion of high strength metals using commercial conform™ machine. *Advance Science Letters*, *19*(3), 701–704. https://doi.org/10.1166/asl.2013.4807.

Zhao, Y., Song, B., Pei, J., Jia, C., Li, B., & Linlin, G. (2013). Effect of deformation speed on the microstructure and mechanical properties of AA6063 during continuous extrusion process. *Journal of Material Processing Technology*, *213*(11), 1855–1863. https://doi.org/10.1016/j.jmatprotec.2013.05.006.

Publisher's Note